
Article:
Liossi, A, Ntountaniotis, D, Kellici, TF et al. (17 more authors) (2017) Exploring the interactions of irbesartan and irbesartan–2-hydroxypropyl-β-cyclodextrin complex with model membranes. Biochimica et Biophysica Acta (BBA) - Biomembranes, 1859 (6). pp. 1089-1098. ISSN 0005-2736

https://doi.org/10.1016/j.bbamem.2017.03.003

Exploring the interactions of irbesartan and irbesartan–2-hydroxypropyl-β-cyclodextrin complex with model membranes

damantia S. Liossi, Dimitrios Ntountaniotis, Tahsin F. Kellici, Maria V. Chatziathanasiadou, Grigorios Megariotis, Maria Mania, Johanna Becker-Baldus, Manfred Kriechbaum, Andraž Krajnc, Eirini Christodoulou, Clemens Glaubitz, Michael Rappolt, Heinz Amenitsch, Gregor Mali, Doros N. Theodorou, Georgia Valsami, Marinos Pitsikalis, Hermis Iatrou, Andreas G. Tzakos, Thomas Mavromoustakos

PII: S0005-2736(17)30077-9
DOI: doi:10.1016/j.bbamem.2017.03.003
Reference: BBAMEM 82442

To appear in: *BBA - Biomembranes*

Received date: 21 November 2016
Revised date: 15 February 2017
Accepted date: 3 March 2017

Please cite this article as: damantia S. Liossi, Dimitrios Ntountaniotis, Tahsin F. Kellici, Maria V. Chatziathanasiadou, Grigorios Megariotis, Maria Mania, Johanna Becker-Baldus, Manfred Kriechbaum, Andraž Krajnc, Eirini Christodoulou, Clemens Glaubitz, Michael Rappolt, Heinz Amenitsch, Gregor Mali, Doros N. Theodorou, Georgia Valsami, Marinos Pitsikalis, Hermis Iatrou, Andreas G. Tzakos, Thomas Mavromoustakos, Exploring the interactions of irbesartan and irbesartan–2-hydroxypropyl-β-cyclodextrin complex with model membranes, *BBA - Biomembranes* (2017), doi:10.1016/j.bbamem.2017.03.003

Exploring the interactions of irbesartan and irbesartan–2-hydroxypropyl-β-cyclodextrin complex with model membranes

*A*damantia S. Liossi[1], Dimitrios Ntountaniotis[1], Tahsin F. Kellici[1,2], Maria V. Chatziathanasiadou[2], Grigorios *M*egariotis[3], Maria Mania[1,4], Johanna Becker-Baldus[5], Manfred Kriechbaum[6], *Andraž* Krajnc[7], Eirini Christodoulou[8], Clemens Glaubitz[5], Michael Rappolt[9], Heinz Amenitsch[6], Gregor Mali[7], Doros N. Theodorou[3], Georgia Valsami[8], Marinos Pitsikalis[1], Hermis Iatrou[1], Andreas G. Tzakos[2], Thomas Mavromoustakos[1,10,*]

[1]Department of Chemistry, National and Kapodistrian University of Athens, Panepistimiopolis Zografou 15771, Greece

[2] Department of Chemistry, University of Ioannina, GR-45110

[3]School of Chemical Engineering, National Technical University of Athens, Athens Greece

[4]Department of Chemistry, University of Patras, Rio 26510, Greece

[5]Institute of Biophysical Chemistry, Goethe University Frankfurt, Max-von-Laue-Str. 9, 60438 Frankfurt, Germany

[6]Institute of Inorganic Chemistry, Graz University of Technology, Stremayrgasse 9/5, A-8010 Graz, Austria.

[7]National Institute of Chemistry, Hajdrihova 19, SI-1001 Ljubljana, Slovenia

[8]Department of Pharmacy, National and Kapodistrian University of Athens, Panepistimiopolis Zografou 15771, Greece

[9]School of Food Science and Nutrition, University of Leeds, Leeds LS2 9JT, UK

[10]Department of Chemistry, York College and the Graduate Center of the City University of New York, 94-20 Guy R. Brewer Blvd., Jamaica, New York, 11451

Keywords: Irbesartan; DPPC; HP-β-CD; Molecular Dynamics; Small Angle X-ray Scattering

***Corresponding author:** T. Mavromoustakos; email: tmavrom@chem.uoa.gr; Tel:+30 2107274475; Fax: +30 2107274761

Abstract

The interactions of irbesartan (IRB) and irbesartan–2-hydroxypropyl-β-cyclodextrin (HP-β-CD) complex with Dipalmitoyl Phosphatidylcholine (DPPC) bilayers have been explored utilizing an array of biophysical techniques ranging from Differential Scanning Calorimetry (DSC), Small angle X-ray Scattering (SAXS), ESI Mass-Spectrometry (ESI-MS) and solid state Nuclear Magnetic Resonance (ssNMR). Molecular Dynamics (MD) calculations have been also conducted to complement the experimental results. Irbesartan was found to be embedded in the lipid membrane core and to affect the phase transition properties of the DPPC bilayers. SAXS studies revealed that irbesartan alone does not display perfect solvation since some coexisting irbesartan crystallites are present. In its complexed form IRB gets fully solvated in the membranes showing that encapsulation of IRB in HP-β-CD may have beneficial effects in the ADME properties of this drug. MD experiments revealed the topological and orientational integration of irbesartan into the phospholipid bilayer being placed at about 1 nm from the membrane centre.

1. Introduction

Angiotensin II type 1 receptor (AT_1R) blockers (ARBs) are recently developed and marketed drugs. These compounds are structural derivatives of the prototype drug losartan and thus belong to the molecular class of sartans. Sartans bear preferentially: (i) a biphenyl ring in which an acidic moiety is attached; (ii) a single or condensed heterocyclic ring and (iii) a hydrophobic group attached to the heterocycle system. It has been proposed that their molecular mechanism of action may involve their insertion and diffusion through lipid bilayers before reaching the AT_1R [1-3].

Although, this class of drugs operate through inhibiting the detrimental action of the octapeptide hormone angiotensin II (Ang II) in pathogenic states, each sartan has a distinct pharmacological profile. This profile is influenced by various properties such as absorption, distribution, half life, dose response and level of AngII antagonism. Taking these properties into account, irbesartan (IRB) (Fig. 1) offers various advantages, in comparison to the other AT_1R antagonists. These advantages are outlined as follows: (i) IRB is well absorbed; (ii) it does not require biotransformation to an active metabolite to exert its antihypertensive activity; (iii) it offers a large volume of distribution; (iv) it has a half-life that is sufficient to allow single-daily dosing; (v) it is associated with a strong and consistent dose-response; (vi) it possesses a statistically superior binding affinity, in an inhibitory mode, for AT_1R, with respect to the majority of ARBs. Adams and Trudeau claim that these pharmacological differences may rationalize the clinical superiority of IRB as compared with, for instance, the prototype molecule losartan [4].

Since AT_1R antagonists suffer from low aqueous solubility, different bilayer pharmaceutical formulations have been patented to overcome this disadvantage [5]. Another way to enhance their low solubility is through formation of inclusion complexes with cyclodextrins (CD). The optimum CD inclusion complex with IRB was found to be 10% (w/v) and the solubility of ionized IRB/γ-CD complex at pH = 7.2 was shown to be three fold greater than that of the unionized complex at pH = 4.3 [6]. In addition, IRB flux via semipermeable membranes increased with increasing γ-CD concentration at both pH values [6]. Hirlekar and Kadam also found out that complexation of IRB with β-CD enhances the solubility by 72.5% and increases more than three times its dissolution rate [7].

Molecular dynamics experiments have been performed with β-CD located either outside or inside lipid bilayers [8]. It was found that β-CD passively diffuses into the lipid bilayer by pointing its wide secondary hydroxyl rim towards the lipid polar groups and then remains at the phosphate and glycerol-ester groups, where it forms hydrogen bonds. The translocation of β-CD deeply inside the hydrophobic region of the lipid bilayer is unfavourable [8]. In a recent review by Gharib et al. it was reported that the encapsulation efficiency of liposomes for hydrophobic drugs was improved for drugs being primarily hosted in cyclodextrins [9].

These findings motivated us to explore the capacity of incorporation and perturbation of IRB in lipid bilayers alone or in a complex form with 2-hydroxypropyl-β-cyclodextrin (HP-β-CD). Particularly, our objective was to shed light on the following points: (a) Can IRB be released from cyclodextrin when it is in the lipid bilayers? (b) If the IRB-HP-β-CD complex is delivered from the aqueous phase, is it still possible for IRB to be released in the lipid bilayers and

behave dynamically in an identical way? (c) If its dynamic behavior is different, what is the driving force generating these alterations? The two different IRB preparations used are illustrated in Fig. 2.

As the model membrane we utilized dipalmitoyl phosphatidylcholine (DPPC) (Fig. 1) since it is commonly used as a simple model membrane system mimicking the plasma bilayers of eukaryotic cells [10]. In a recent review it has also been reported that DPPC is one of the most commonly used phospholipids in the preparation of liposomes for entrapping CD inclusion complexes [9]. Cyclodextrin was used since it is known to promote the drug transport to its active site and therefore increases its pharmacological potential [6, 11-14]. We specifically selected, herein, 2-hydroxypropyl-β-cyclodextrin (HP-β-CD) (Fig. 1), since it has been reported to be devoid of any toxicity [15-17]. To characterize these complexes and to understand the nature of these interactions, we applied a combined array of biophysical techniques consisting of Differential Scanning Calorimetry (DSC), ESI Mass Spectrometry (ESI-MS), Small Angle X-ray Scattering (SAXS), solid state Nuclear Magnetic Resonance (ssNMR) and Molecular Dynamics (MD). To our knowledge this is the first attempt to compare the topology and associated effects of a drug in lipid bilayers both in its encapsulated with cyclodextrin form and in its unencapsulated form.

The obtained results do not only provide information regarding the mode of action of IRB at molecular level, but also project insights on new drug delivery routes that can potentially offer optimized ADME for this drug [6, 10-14].

2. Materials and Methods

2.1. Materials

IRB was kindly provided by Prof. M. Koupparis. DPPC was purchased from Avanti Polar Lipids Inc. (Alabaster, AL). Deuterium depleted water and HP-β-CD were purchased from Sigma Aldrich (St. Louis, MO).

2.1.1. Sample preparation

Preparation of the IRB–HP-β-CD lyophilized complex: A freeze-drying procedure was applied for the preparation of IRB–HP-β-CD lyophilized product. For the preparation of IRB–HP-β-CD aqueous solutions for freeze-drying in a molar ratio of 1:2, the neutralization method was used [18]. More specifically, 0.060 g of irbersartan and 0.408 g of HP-β-CD were weighed accurately, transferred in a 100 mL beaker and suspended with 50 mL of water. Small amounts of ammonium hydroxide were then added under continuous stirring and pH monitoring until complete dissolution and pH adjustment to a value between 9 and 10 have been obtained. The resulting solution at molar ratio of 1:2 was thereafter frozen at -80 ^{o}C and freeze-dried using a Kryodos-50 model Telstar lyophilizer.

Preparation of liposome mixture: DPPC and IRB stock solutions were prepared by dissolving weighted amounts of dry lipid and IRB powder in chloroform. The drug concentrations used were x = 0.05 (5 mol%) or x=0.2 (20 mol%). Appropriate amounts of drug in a pure or complexed form with HP-β-CD was used in the mixtures. The organic DPPC/IRB, or DPPC/complex IRB–HP-β-CD were then evaporated at room temperature under a gentle stream of nitrogen and thereafter placed under vacuum for 12 hours in order to form a thin lipid film at the bottom of glass vials. The obtained mixtures were then fully hydrated (50% wt/wt deuterium depleted water) in order to achieve multilamellar vesicles (MLVs).

Alternatively, complexed IRB–HP-β-CD compounds were added to the aqueous phase of readily formed DPPC MLVs dispersions (see Fig. 1).

2.2. Methods

2.2.1. Differential scanning calorimetry

The prepared samples for DSC were transferred to stainless steel capsules obtained from Perkin-Elmer and sealed. Thermal scans were obtained on a TA instrument MDSC Model 2910 (De, USA). All samples were scanned from 10 to 60 °C at least three times until identical thermal scans were obtained using a scanning rate of 2.5 °C/min. The temperature scale of the calorimeter was calibrated using indium (T_m = 156.6 °C) and DPPC bilayers (T_m = 41.2 °C). The following diagnostic parameters were used for the study of drug to membrane interactions: T_m (maximum position of the recorded heat capacity), T_{onset} (the starting temperature of the phase transition) and the respective parameters concerning the pre-transition. The area under the peak represents the enthalpy change during the transition (ΔH). The mean values of ΔH of three identical scans were tabulated. The IRB concentrations used for the different experiments were 5, 10 and 20 mol%.

2.2.2. Solid-state ^{13}C CP/MAS NMR spectroscopy

^{13}C cross polarization/magic-angle spinning (^{13}C CP/MAS) solid-state NMR spectra were recorded on a Varian 600 MHz spectrometers equipped with a 3.2 mm HX MAS probe. Approximately 20 mg of each sample was packed tightly into a zirconia rotor and spun at 5 kHz. The duration of the CP block in the CP/MAS experiment was 5 ms, repetition delay between scans was 2 s, and

number of scans was 400. The ^{13}C chemical shift axis was referenced to tetramethylsilane.

For the sample DPPC/HP-β-CD (x=0.20) ^{13}C CP/MAS and MAS spectra were recorded at sample rotation frequency of 15 kHz. The spectra were recorded on a Bruker 600 MHz spectrometer equipped with a 4 mm HX MAS probe. Approximately 50 mg of each sample was packed tightly into a zirconia rotor. Cross-polarization was used for ^{13}C excitation using an 80% linear ramp. During ^{13}C detection, 100 kHz Spinal-64 proton decoupling was applied [19-21]. The number of scans used in the experiment was 1000.

2.2.3. X-ray diffraction experiments

Small angle X-ray scattering (SAXS) measurements were performed with a high-flux SAXSess camera (Anton Paar, Graz, Austria) connected to a Debyeflex 3003 X-ray generator (GE-Electric, Germany), operating at 40 kV and 50 mA with a sealed-tube Cu anode. The Goebel-mirror focused and Kratky-slit collimated X-ray beam was line shaped (17 mm horizontal dimension at the sample) and scattered radiation was measured in the transmission mode and recorded by a one-dimensional MYTHEN-1k microstrip solid-state detector (Dectris Switzerland), within a q-range (with q being the magnitude of the scattering vector) of 0.01 to 0.5 $Å^{-1}$. Using Cu Kα radiation of wavelength 1.54 Å and a sample-to-detector distance of 307 mm this corresponds to a total 2θ region of 0.14° to 7°, applying the conversion $q\ [A^{-1}] = 4\pi(\sin\theta)/\lambda$ with 2θ being the scattering angle with respect to the incident beam and λ the wavelength of the X-rays. Samples were filled into a 1 mm (diameter) reusable quartz capillary (wall thickness of 10 µm) with

vacuum-tight sealing screw-caps at both ends. All measurements of the samples in the capillary were done in vacuum and at the respective temperatures with an exposure time of 10 min at each temperature step in a heating scan (20° to 50°C in 5° intervals with 10 min equilibration).

2.2.4. Molecular dynamics

The CHARMM 36 force field [22, 23] was employed for the simulation of a fully hydrated DPPC bilayer at the atomistic level while the water phase was described by the well-known transferable intermolecular potential 3 point (TIP3P) model [24]. As far as the initial configuration of the bilayer is concerned, it was downloaded from the web-page of the Laboratory of Molecular and Thermodynamic Modeling at the University of Maryland. The topology files for IRB and the CD derivative were created with the SwissParam server program [25]. The latter choice is justified as follows: SwissParam provides topology files in GROMACS format based on Merck molecular force field (MMFF) in a functional form that is in compatibility with the CHARMM force field. It should also be mentioned that MMFF reproduces accurately bond lengths, bond angles and vibrational frequencies in comparsion with experimental data as well as treating correctly conformational energetics [26]. Another reason for choosing the SwissParam server was the extensive number of successful tests for organic molecules reported in references [25, 26]. Also, according to reference 25, further optimization of the force-field parameters may be needed for highly accurate calculations of complex organic molecules. All molecular dynamics (MD) simulations were conducted with the GROMACS 5.1.1 package [27] in the NP_ZAT ensemble with a constant area, A, being equal to 0.64 nm^2/lipid, while the

equations of motion were integrated with a time step of 1 fs. The temperature and pressure along the Z-axis were kept constant at 323K and 1bar, respectively, by employing the Berendsen thermostat and barostat [28]. Long-range electrostatic interactions were treated with the particle mesh Ewald (PME) method [29], while Lennard-Jones interactions were calculated using a 1.2 nm cut-off radius. The forces were smoothly switched to zero between a distance of $r_{vdw\text{-}switch}$=1.0 nm and the previously-mentioned cut-off radius by applying the force-switch option of GROMACS package. Two different concentrations of IRB molecules were simulated in the lipid membrane, i.e.: 1.4 mol.%, 12.2mol.%. The complex formed by IRB and HP-β-CD was created in an aqueous phase containing 13284 water molecules. The membrane under study contained 72 DPPC molecules in contact with 2162 water molecules. These two systems were initially energy-minimized using the steepest descent method, and subsequently MD simulations were conducted for 0.5 μs. The same membrane was employed in the presence of IRB–HP-β-CD, but in this case the aqueous phase contained 3604 water molecules. The total duration of the IRB–HP-β-CD–DPPC MD simulation was 1μs. In addition, a set of 29 umbrella sampling simulations were performed for the computation of the potential of mean force (PMF) of the IRB from lipid to water phase by employing the weighted histogram analysis method (WHAM) [30]. In particular, the Z-axis was selected to be the reaction coordinate, ζ, the bilayer centre corresponding to the value ζ=0.0 nm. The duration of the biasing simulations was 85 ns, of which the first 35 ns were regarded as equilibration and therefore were discarded. The protocol applied for the computation of PMF was according to that of the reference 39 and references therein.

2.2.5 ESI-MS measurements

The EVOQ™ Elite ER LC-TQ system, triple quadrupole mass spectrometer was used to perform full scan analysis of the HP-β-CD and IRB–HP-β-CD complex. Each of them (0.1mg) was diluted in distilled H_2O (LC-MS grade, Fisher) and injected directly to the spectrometer. The measurement was performed in negative ionization mode, using an ESI probe. Spray voltage (-) was set to 4000 V, heated probe gas flow to 0 units, heated probe temperature at 40 °C, cone gas flow to 20 units, cone temperature at 300 °C and nebulizer gas flow to 20 units. Results were collected through the MSWS software, provided by Bruker.

3. Results and Discussion

3.1 Differential scanning calorimetry

Pure fully hydrated DPPC bilayers (Fig. SF1A, Table 1) show two characteristic endothermic peaks, the pre- and the main transition, respectively. Below the pretransition the DPPC molecules form the well-organized lamellar gel phase, $L_{\beta'}$, while above the main transition temperature a fluid lamellar phase, L_{α}, is apparent. An intermediate phase, $P_{\beta'}$, is also observed, in which the bilayers are modulated by a periodic ripple (ripple phase) [31]. The recorded transition temperatures and enthalpies are in good agreement with literature [32].

The presence of 20% mol of IRB results in a reduction of the T_m and narrowing of the transition width of the main phase transition (Fig. SF1B). IRB abolishes the pre-transition indicating a strong effect on the head-group region of lipid bilayers, while it does not affect ΔH considerably (Table 1).

HP-β-CD does not cause significant changes on DPPC bilayers (Fig. SF1C). Both pre-transition and main phase transition are conserved, however, shifted to lower temperatures and the enthalpy, ΔH, is reduced too. When the complex is provided from the aqueous phase to the readily formed DPPC MLVs, then T_m was observed about 2 °C lower (Fig. SF1D), and also ΔH of this sample was determined to be lower than that of pure DPPC bilayers.

MLV derived after hydration of DPPC and IRB–HP-β-CD complex in the lipid film form displayed in the DSC scan 1.3 °C lower T_m as compared to pure DPPC bilayers and similar ΔH (Fig. SF1E). The above thermal profiles show that DPPC bilayers containing IRB–HP-β-CD complex provided outside or included inside during the preparation that IRB is released and perturbs the lipid bilayers.

3.2. Small angle X-ray scattering

DPPC bilayers in the gel phase show four distinct diffraction orders indicating a high stacking order of the phospholipid membranes. At temperatures between the pretransition and main transition corrugated bilayers with a periodic ripple and hexagonal chain packing are formed. This is seen as a broadening of the reflections. In the liquid crystalline phase, a sharpening of the peaks and an increase in intensity is seen, typical for the reformation of planar lipid bilayers (Fig. 3A).

As seen in the relatively broad diffraction peaks the stacking of the DPPC/IRB bilayers is less ordered as compared to pure DPPC bilayers (Fig. 3B). While in the gel-phase regime (20-40 °C) only a slightly higher repeat is apparent (Figure 4), in the liquid crystalline phase only spatially uncorrelated membranes are observed

(45-55 °C), i.e. the bilayers unbind. Further, IRB suppresses the formation of the ripple phase as confirmed from the DSC measurements. Most strikingly, above the main transition temperature only diffuse scattering arising from spatially uncorrelated bilayers is observed. A consistent explanation would be that the incorporation of IRB in the L_α phase leads to an increase in fluidization of the hydrocarbon chains causing stronger bilayer undulations, and finally provokes the unbinding of the membranes. Although IRB strongly interacts with DPPC bilayers over the entire studied temperature range, we note that IRB is not totally solvated in the bilayers, since a strong diffraction peak at q = 0.335 $Å^{-1}$ is clearly visible throughout the entire temperature range (marked with * in Fig. 3B). This diffraction peak stems most probably from precipitated IRB aggregating in the crystal A form [33].

The incorporation of HP-β-CD in DPPC bilayers does not suppress any phase formation, but a broadening of the diffraction peaks is observed in all three phases (Fig. 3C). This indicates that the stacking of the lipid bilayers is not as ordered as with pure DPPC bilayers. In accordance to the DSC data, both the pretransition and main transition are lowered by a few degrees, and it is tempting to assume that the HP-β-CD incorporation decreases the packing density of the lipids. This would in turn lead bilayers with a decreased bending modulus, and hence explain the reduced quasi long-range order of the membrane stacking as confirmed by the broadening of the diffraction peaks.

When the IRB–HP-β-CD complex is added to the excess of water layer, and subsequently interacts with the DPPC bilayers, only in the $L_{\beta'}$ phase broad diffraction peaks are apparent (Fig. 3D: 20-25 °C). From 30 °C onwards merely

diffuse scattering arising from spatially uncorrelated membranes are observed. When the IRB–HP-β-CD complex was in dry lipid film mixture with DPPC and then hydrated, the fluidization effect of the membranes is maximized as it can be observed by the increase breadth of the spectra profiles (Fig. 3E).

3.3. Solid state NMR spectroscopy

3.3.1. HP-β-CD in DPPC bilayers

^{13}C CP/MAS experiments using phospholipid bilayers both in gel and liquid crystalline phases have been used to examine the effect of HP-β-CD on DPPC bilayers. Two kinds of experiments have been performed at ambient temperature: (a) In the first experiment HP-β-CD has been co-dissolved with DPPC in chloroform, evaporated, dried and hydrated to form fully hydrated multilamellar vesicles (Figure 2A); (b) In the second experiment HP-β-CD was added to the aqueous phase of DPPC prepared multilamellar vesicles (Figure 2B). The obtained spectra showed almost no additional peaks attributed to HP-β-CD. As in both methods the spectra were identical, we proceeded obtaining ^{13}C CP/MAS spectra using the first methodology at three temperatures (25-45 °C) to cover all mesomorphic states of DPPC bilayers. Again, the peaks of HP-β-CD were barely observable (Figure 5 and Fig. SF2). The absence of cross polarization between HP-β-CD and phospholipid DPPC presumably shows that the former molecule sits on the surface of the lipid bilayers and that the distances between the ^{1}H and ^{13}C nuclei of the two species are thus sufficiently large or that the dynamics of the HP-β-CD is sufficiently fast, so that the ^{1}H-^{13}C (residual) dipolar interaction is practicaly negligible. ^{13}C MAS experiments confirmed this preposition as the peaks attributed to (HP-β-CD) are eminent at 15 °C (Figure 6).

These results are in agreement with those of DSC, which showed only small effect of HP-β-CD on DPPC bilayers. Small effect of HP-β-CD on DPPC bilayers were also reported previously. HP-β-CD was among the least perturbing CDs used in the studies performed by Nishuo et al. [34, 35].

3.3.2. Irbesartan in DPPC bilayers

DPPC bilayers containing IRB at the three different temperatures of 25 °C, 35 °C and 45 °C, covering all mesomorphic states of the phospholipid bilayers, were also inspected by NMR. As it can be observed from Tables ST1 and ST2 the chemical shifts of the carbons presenting the phospholipid bilayers have not been modified significantly due to the presence of the drug. Additional peaks due to the drug attributed to its flexible and rigid segments have been observed. The aromatic region of the drug consists of peaks characterized by increased linewidth, an indication that this region of the lipid bilayers is squeezed into the lipid bilayers with restrained flexibility. C31 and C30 belonging to the butyl chain of the drug are clearly seen in all temperature range (25-45 °C) [36]. Thus, the butyl chain of IRB is embedded in a more flexible hydrophobic core of phospholipid bilayers compared to the aromatic region. However, the peaks are still broad designating restraint in the lipid core. C4 is also observable at the temperature range in which the experiments were conducted. This evidence that the cyclopentyl ring of 1,3-diazaspiro[4.4]non-1-en-4-one is embedded deep in the hydrophobic core of the lipid bilayers, a more flexible segment. C6-C9 carbons of the cyclopentyl ring are restrained into the lipid bilayers and do not appear in the spectra. Another reason for not observing these peaks may be their coincidence with the peaks of phospholipid aliphatic area. The amide carbonyl group of 1,3-diazaspiro[4.4]non-

1-en-4-one is clearly discernible at 25 °C but not observable at 35 °C and 45 °C showing its dependence on the fluidity of the lipid bilayers (Figure 5, Figure SF2).

3.3.3. Irbesartan complex with HP-β-CD in DPPC bilayers

Two kinds of experiments have been conducted. In the first experiment the complex is included as a mixture with DPPC and subsequently hydrated (Figure 2A) In the second preparation, the complex of the drug was added from outside (Figure 2B).

In the first kind of experiments using cross polarization and temperature range of 25-45 °C signals of the drug molecule are very broad (Fig. 5 and Fig. SF2). Peaks of HP-β-CD are not observed showing again that cyclodextrin is located at the surface of the lipid bilayers. When MAS experiment was performed at 45 °C, thus without using cross polarization (see supporting information), peaks attributed to cyclodextrin are clearly seen proving again that cyclodextrin is localized on the surface of the lipids bilayers. In the second kind of experiments using again cross polarization and temperature range of 25-45 °C the signals of the drug molecule are very broad.

3.4. Molecular dynamics

This section begins with the detailed analysis of the PMF of IRB from lipid to water phase, which is depicted in SF3(a). At large distances, the curve in question approaches a constant value corresponding to the value in the water phase. Regarding the position of the minimum, it is located approximately 1.0 nm from the bilayer center, while the free-energy barrier for a drug molecule to jump from one leaflet of the membrane to the opposite one is 28.5kJ/mol. This rather high

value indicates that crossing events are not easily realizable and may not be observed during MD simulations of duration on the order of hundreds of ns. Moreover, one can compute from such a curve the free-energy difference of partitioning into the membrane as the difference between the PMF value at large distances (>2.5 nm) and the PMF value at the minimum. This free-energy difference is approximately 33.5 kJ/mol. Another interesting feature of the curve of SF3(a) is the existence of a linear region (1.5-2.3 nm) indicating a large attractive force toward the interior of the lipid membrane. The slope of this linear region is estimated as 30.5 kJ/mol/nm by applying a linear least-squares fit. In addition, an analysis of errors was applied in the computed PMF. This analysis was based on the WHAM utility of GROMACS which is described in detail in reference 30; the statistical uncertainty, given by the standard deviation [30], is estimated by using boostrap analysis [37]. More specifically, the errors in the PMF were computed as a function of the selected reaction coordinate. These errors are visualized as errorbars in Figure SF3(b) with all errorbars being less than 2.4 kJ/mol. An interesting study of technical issues (e.g. dependence of errors on the position along the reaction coordinate) of umbrella sampling and metadynamics is that of reference [38]. As far as the unbiased MD simulations are concerned, one IRB molecule was initially placed in the water phase and the whole system was energy minimized using the steepest descent method [28]. A graphical representation of this system is provided in Figure 7A, in which the IRB is visualized with green contour after its insertion into the lipid phase. SF4(a) shows the temporal evolution of the Z-coordinate of the IRB center of mass (green color) along with the Z-coordinates of DPPC phosphorus centers of mass (black color)

for the two leaflets of the lipid membrane. It is observed that, after nearly 11ns of MD simulation, the IRB molecule was inserted in the bilayer and thus during this time interval the green dots are not found in the intermediate area delimited by the black curves. In the rest of this simulation, no crossing events were recorded and this means that the free-energy barrier (see Figure SF3(a)) for hopping between the two leaflets was not overcome. Moreover, the IRB center of mass is fluctuating around 1nm from the bilayer center, as expected from the minimum value of the PMF. Having established that IRB prefers being inserted in the bilayer, a higher concentration (12.2%) was also simulated by placing the drug molecules inside the hydrophobic core of the lipid phase. Again the NP_zAT ensemble was used, with the area per lipid set to 0.64nm^2. This choice is justified by experimental results presented in an older study concerning the candesartan cilexetil, another molecule belonging to the class of sartans [39]. More specifically, the area per lipid up to concentrations of 12% varies from 0.645 to 0.630 nm^2. The temporal evolution of the Z-coordinate of the IRB center of mass, in the case of the highest concentration, is depicted in SF4(b) with each drug molecule being visualized by a different color. Again no crossing event was observed during the 0.5μs of the production run. Moreover, the density profiles along the Z-axis for the same system are provided in Figure 7B. The drugs are distributed symmetrically in the two leaflets, whereas the peak values are in accordance with the PMF. One representative conformation of IRB inside the bilayer, as estimated by applying a clustering algorithm that is available in the USCF chimera software [40], is given in Figure 8. The axes of the simulation box are also included in the

aforementioned figure for a better understanding of the relative position of the IRB with respect to the characteristic direction of the Z-axis.

Now we turn our attention to the formation of the complex IRB–HP-β-CD. To this end, IRB and the CD derivative were placed in a water phase described by the TIP3P model at an initial distance greater than 2.0 nm. Our aim was the spontaneous creation of the complex under the employed force-field (see also the simulation details section). Indeed, the IRB–HP-β-CD complex was created within the first ten nanoseconds of a 140 ns MD simulation. After the formation of the complex and making use of the pairdist utility of GROMACS, the distance between the centers of mass of the two molecules in the bound state is (0.649±0.004) nm. Next, the last IRB–HP-β-CD configuration of this MD simulation was placed in the water phase surrounding the lipid bilayer of 72 DPPC molecules. The time evolution of the IRB–HP-β-CD is monitored in terms of the Z-coordinate of its two constituent molecules. As seen in SF5, the complex enters the membrane after nearly 40 ns of MD simulation. Another interesting conclusion from the aforementioned figure is that the IRB is located deeper in the membrane with respect to the CD derivative which fluctuates asymmetrically around the positions of phosphorus atoms of one DPPC leaflet. A complementary view of this system is provided in Figure 7D in which density profiles along the Z-axis of various components are depicted with different colours. This diagram is taken from the last 0.25 μs of the MD simulation and the abscissa is extended to higher values in comparison to those of Figure 7B, since an extended water phase is employed in this case. The IRB–HP-β-CD density profile is visualized in green colour, whilst the profile concerning IRB itself is separately depicted with red

colour. A graphical representation of the system under study is given in Figure 7C with the CD derivative and IRB shown in black and blue colours, respectively. It is also seen from this figure that IRB is oriented towards the interior of the membrane and the CD derivative is located at the water-DPPC interface.

3.5 ESI-Mass spectrometry studies

To qualitatively asses the species present in the IRB–HP-β-CD complex ESI mass-spectroscopy was utilized (Fig. 9). This technique has been formerly used to monitor weak non-covalent interactions such as the supramolecular interactions of HP-β-CD with losartan [41] and progesterone [42].

Fig. 9A illustrates the mass spectrum of HP-β-CD. In this spectrum a distribution of peaks is observed with m/z between 1400.00 and 1650.00, with the following three peaks with m/z 1447.70, 1483.80 and 1541.7 that have been used in the characterization of the complex that follows. Such broad distribution has been attributed due to the presence of a mixture of different cyclodextrins bearing different degree of substitution in HP-β-CD [41]. In Fig. **9B** the ESI-MS spectrum of the IRB–HP-β-CD complex is presented. At m/z values localized between 1800 and 2000 three peaks are observed, 1853.10, 1911.40 and 1968.70, relating to three types of inclusion compounds with stoichiometry 1:1. The relevant result could be attributed to the formation of a stable complex driven by hydrophobic interactions as supported by the complementary techniques used in this work, similar to the case of the reported complex of losartan with HP-β-CD REF 41. This is in contrast to the case of the reported complex of progesterone with β-CD or HP-β-CD where different and higher complex ratios could be monitored [42]. These higher complex ratios have been hypothesized to be formed due to

nonspecific interactions of β-CD or HP-β-CD with progesterone rather than hydrophobic inclusion.

4. Conclusions

IRB is a marketed drug with a well known antihypertensive activity and other beneficial effects. Its mode of action may be strongly related to its membrane incorporation and subsequent diffusion to the active site of the AT_1R. Due to IRB's high lipophilicity its formulation with HP-β-CD may improve its pharmacological profile. It is therefore of great importance to study its interactions with model membranes both in its complexed form with HP-β-CD as also in its unencapsulated form. Herein, two formulations have been evaluated: (i) either a 1:1 complex of HP-β-CD with IRB, as characterized by ESI MS, was added to the aqueous phase of the MLV dispersions or (ii) mixed DPPC/IRB–HP-β-CD (4:1) complex films were hydrated.

The thermal changes observed using the macroscopic method of DSC suggest: (a) HP-β-CD does not exert strong effect in DPPC bilayers, but it sits on the surface. This observation is strongly supported by the microscopic method of ssNMR spectroscopy. ^{13}CP/MAS experiments showed no additional peaks due to HP-β-CD, peaks that were evident when cross polarization was not applied. (b) Irbesartan is inserted in DPPC bilayers where it modifies significantly the thermal profile of pure DPPC bilayers. MD experiments confirm DSC results and provide complementary information on the localization of the molecule. Information on the localization of irbesartan in DPPC bilayers is obtained also through ssNMR. Clearly, broad peaks of the aromatic segments of irbesartan are observed,

signifying that they are intercalating well in the bilayer's hydrophobic region and this reduces the mobility of the alkyl chains. In addition, all segments of irbesartan are intercalated with different mobility as it is shown by the ^{13}CP/MAS experiments. X-ray diffraction data also complement results from ssNMR, DSC and MD as they show not only strong interactions between irbesartan and DPPC bilayers, but also its inability for full solvation. (c) Interestingly, different modes of delivery of IRB to model membranes, unencapsulated or IRB–HP-β-CD encapsulated, exerted significant differences on the membrane internalization as depicted by DSC, solid state NMR spectroscopy, X-ray diffraction and Molecular Dynamics. Only in its complexed form IRB gets fully solvated in the membranes, whereas the pure IRB/DPPC interactions led to the additional formation of IRB crystals. These results highlight that encapsulation of IRB in HP-β-CD may have beneficial effects in the ADME properties of this drug.

Acknowledgements

This work was supported by CERIC funded programme (proposal number 20152002), programme for the promotion of the exchange and scientific cooperation between Greece and Germany IKYDA 2015 and by the Cy-Tera Project (NEA ΥΠΟΔΟΜΗ/ΣΤΡΑΤΗ/0308/31), which is co-funded by the European Regional Development Fund and the Republic of Cyprus through the Research Promotion Foundation. Grigorios Megariotis and Doros N. Theodorou thank the Limmat Foundation for the financial support. Part of their research has been co-financed by the European Union (European Social Fund-ESF) and Greek national funds through the Operational Programme 'Education and Lifelong Learning' of the National Strategic Reference Framework (NSRF)-Research Funding Programme: THALIS. Investing in knowledge society through the European social fund [grant number MIS 379436]. This work was supported by computational time granted from the Greek Research & Technology Network (GRNET) in the National HPC facility –ARIS- under project IDs pr001042 (MultiCLC) and pr002023 (HMSM).

References

[1] T.F. Kellici, A.G. Tzakos, T. Mavromoustakos, Rational drug design and synthesis of molecules targeting the angiotensin II type 1 and type 2 receptors, Molecules, 20 (2015) 3868-3897.

[2] J. Tamargo, J. Duarte, L.M. Ruilope, New antihypertensive drugs under development, Curr. Med. Chem., 22 (2015) 305-342.

[3] T.F. Kellici, D. Ntountaniotis, E. Kritsi, M. Zervou, P. Zoumpoulakis, C. Potamitis, S. Durdagi, R.E. Salmas, G. Ergun, E. Gokdemir, M. Halabalaki, I.P. Gerothanassis, G. Liapakis, A. Tzakos, T. Mavromoustakos, Leveraging NMR and X-ray Data of the Free Ligands to Build Better Drugs Targeting Angiotensin II Type 1 G-Protein Coupled Receptor, Curr. Med. Chem., 23 (2016) 36-59.

[4] M.A. Adams, L. Trudeau, Irbesartan: review of pharmacology and comparative properties, Can. J. Clin. Pharmacol., 7 (2000) 22-31.

[5] T.F. Kellici, G. Liapakis, A.G. Tzakos, T. Mavromoustakos, Pharmaceutical compositions for antihypertensive treatments: a patent review, Expert Opin. Ther. Pat., 25 (2015) 1305-1317.

[6] P. Jansook, C. Muankaew, E. Stefansson, T. Loftsson, Development of eye drops containing antihypertensive drugs: formulation of aqueous irbesartan/gammaCD eye drops, Pharm. Dev. Technol., 20 (2015) 626-632.

[7] R. Hirlekar, V. Kadam, Preformulation study of the inclusion complex irbesartan-beta-cyclodextrin, AAPS PharmSciTech, 10 (2009) 276-281.

[8] W. Khuntawee, P. Wolschann, T. Rungrotmongkol, J. Wong-Ekkabut, S. Hannongbua, Molecular Dynamics Simulations of the Interaction of Beta Cyclodextrin with a Lipid Bilayer, J. Chem. Inf. Model., 55 (2015) 1894-1902.

[9] R. Gharib, H. Greige-Gerges, S. Fourmentin, C. Charcosset, L. Auezova, Liposomes incorporating cyclodextrin-drug inclusion complexes: Current state of knowledge, Carbohydr. Polym., 129 (2015) 175-186.

[10] D. Ntountaniotis, T. Kellici, A. Tzakos, P. Kolokotroni, T. Tselios, J. Becker-Baldus, C. Glaubitz, S. Lin, A. Makriyannis, T. Mavromoustakos, The application of solid-state NMR spectroscopy to study candesartan cilexetil (TCV-116) membrane interactions. Comparative study with the AT1R antagonist drug olmesartan, Biochim. Biophys. Acta, 1838 (2014) 2439-2450.

[11] Q.F. Zhang, H.C. Nie, X.C. Shangguang, Z.P. Yin, G.D. Zheng, J.G. Chen, Aqueous solubility and stability enhancement of astilbin through complexation with cyclodextrins, J. Agric. Food Chem., 61 (2013) 151-156.

[12] N.M. Patro, A. Sultana, K. Terao, D. Nakata, A. Jo, A. Urano, Y. Ishida, R.N. Gorantla, V. Pandit, K. Devi, S. Rohit, B.K. Grewal, E.M. Sophia, A. Suresh, V.K. Ekbote, S. Suresh, Comparison and correlation of in vitro, in vivo and in silico evaluations of alpha, beta and gamma cyclodextrin complexes of curcumin, J. Incl. Phenom. Macrocycl. Chem., 78 (2014) 471-483.

[13] C. Danciu, C. Soica, M. Oltean, S. Avram, F. Borcan, E. Csanyi, R. Ambrus, I. Zupko, D. Muntean, C.A. Dehelean, M. Craina, R.A. Popovici, Genistein in 1:1 inclusion complexes with ramified cyclodextrins: theoretical, physicochemical and biological evaluation, International journal of molecular sciences, 15 (2014) 1962-1982.

[14] E. Dreassi, A.T. Zizzari, M. Mori, I. Filippi, A. Belfiore, A. Naldini, F. Carraro, A. Santucci, S. Schenone, M. Botta, 2-Hydroxypropyl-beta-cyclodextrin

strongly improves water solubility and anti-proliferative activity of pyrazolo[3,4-d]pyrimidines Src-Abl dual inhibitors, Eur. J. Med. Chem., 45 (2010) 5958-5964.

[15] T.F. Kellici, D. Ntountaniotis, G. Leonis, M. Chatziathanasiadou, A.V. Chatzikonstantinou, J. Becker-Baldus, C. Glaubitz, A.G. Tzakos, K. Viras, P. Chatzigeorgiou, S. Tzimas, E. Kefala, G. Valsami, H. Archontaki, M.G. Papadopoulos, T. Mavromoustakos, Investigation of the interactions of silibinin with 2-hydroxypropyl-beta-cyclodextrin through biophysical techniques and computational methods, Mol. Pharm., 12 (2015) 954-965.

[16] T.F. Kellici, M.V. Chatziathanasiadou, D. Diamantis, A.V. Chatzikonstantinou, I. Andreadelis, E. Christodoulou, G. Valsami, T. Mavromoustakos, A.G. Tzakos, Mapping the interactions and bioactivity of quercetin-(2-hydroxypropyl)-beta-cyclodextrin complex, Int. J. Pharm., 511 (2016) 303-311.

[17] M. Malanga, J. Szemán, É. Fenyvesi, I. Puskás, K. Csabai, G. Gyémánt, F. Fenyvesi, L. Szente, "Back to the Future": A New Look at Hydroxypropyl Beta-Cyclodextrins, J. Pharm. Sci., 105 (2016) 2921-2931.

[18] A. Figueiras, R.A. Carvalho, L. Ribeiro, J.J. Torres-Labandeira, F.J. Veiga, Solid-state characterization and dissolution profiles of the inclusion complexes of omeprazole with native and chemically modified beta-cyclodextrin, Eur. J. Pharm. Biopharm., 67 (2007) 531-539.

[19] A.K. Chattah, K.H. Mroue, L.Y. Pfund, A. Ramamoorthy, M.R. Longhi, C. Garnero, insights into novel supramolecular complexes of two solid forms of norfloxacin and beta-cyclodextrin, J. Pharm. Sci., 102 (2013) 3717-3724.

[20] T. Fukami, T. Ishii, T. Io, N. Suzuki, T. Suzuki, K. Yamamoto, J. Xu, A. Ramamoorthy, K. Tomono, Nanoparticle processing in the solid state dramatically increases the cell membrane permeation of a cholesterol-lowering drug, probucol, Mol. Pharm., 6 (2009) 1029-1035.

[21] T. Io, T. Fukami, K. Yamamoto, T. Suzuki, J. Xu, K. Tomono, A. Ramamoorthy, Homogeneous nanoparticles to enhance the efficiency of a hydrophobic drug, antihyperlipidemic probucol, characterized by solid-state NMR, Mol. Pharm., 7 (2010) 299-305.

[22] J.B. Klauda, R.M. Venable, J.A. Freites, J.W. O'Connor, D.J. Tobias, C. Mondragon-Ramirez, I. Vorobyov, A.D. MacKerell, Jr., R.W. Pastor, Update of the CHARMM all-atom additive force field for lipids: validation on six lipid types, J. Phys. Chem. B, 114 (2010) 7830-7843.

[23] R.W. Pastor, A.D. Mackerell, Jr., Development of the CHARMM Force Field for Lipids, J. Phys. Chem. Lett., 2 (2011) 1526-1532.

[24] W.L. Jorgensen, J. Chandrasekhar, J.D. Madura, R.W. Impey, M.L. Klein, Comparison of simple potential functions for simulating liquid water, J. Chem. Phys, 79 (1983) 926-935.

[25] V. Zoete, M.A. Cuendet, A. Grosdidier, O. Michielin, SwissParam: a fast force field generation tool for small organic molecules, J. Comput. Chem., 32 (2011) 2359-2368.

[26] T.A. Halgren, Merck molecular force field. I. Basis, form, scope, parameterization, and performance of MMFF94, J. Comput. Chem., 17 (1996) 490-519.

[27] B. Hess, C. Kutzner, D. van der Spoel, E. Lindahl, GROMACS 4: Algorithms for Highly Efficient, Load-Balanced, and Scalable Molecular Simulation, J. Chem. Theory Comput., 4 (2008) 435-447.

[28] H.J.C. Berendsen, J.P.M. Postma, W.F. van Gunsteren, A. DiNola, J.R. Haak, Molecular dynamics with coupling to an external bath, J. Chem. Phys, 81 (1984) 3684-3690.

[29] U. Essmann, L. Perera, M.L. Berkowitz, T. Darden, H. Lee, L.G. Pedersen, A smooth particle mesh Ewald method, J. Chem. Phys, 103 (1995) 8577-8593.

[30] J.S. Hub, B.L. de Groot, D. van der Spoel, g_wham—A Free Weighted Histogram Analysis Implementation Including Robust Error and Autocorrelation Estimates, J. Chem. Theory Comput., 6 (2010) 3713-3720.

[31] M.J. Janiak, D.M. Small, G.G. Shipley, Nature of the thermal pretransition of synthetic phospholipids: dimyristoyl- and dipalmitoyllecithin, Biochemistry, 15 (1976) 4575-4580.

[32] R. Koynova, M. Caffrey, Phases and phase transitions of the phosphatidylcholines, Biochim. Biophys. Acta, 1376 (1998) 91-145.

[33] Z. Bocskei, K. Simon, R. Rao, A. Caron, C.A. Rodger, M. Bauer, Irbesartan Crystal Form B, Acta Crystallographica Section C, 54 (1998) 808-810.

[34] J. Nishijo, H. Mizuno, Interactions of cyclodextrins with DPPC liposomes. Differential scanning calorimetry studies, Chem. Pharm. Bull. (Tokyo), 46 (1998) 120-124.

[35] J. Nishijo, S. Shiota, K. Mazima, Y. Inoue, H. Mizuno, J. Yoshida, Interactions of cyclodextrins with dipalmitoyl, distearoyl, and dimyristoyl phosphatidyl choline liposomes. A study by leakage of carboxyfluorescein in inner

aqueous phase of unilamellar liposomes, Chem. Pharm. Bull. (Tokyo), 48 (2000) 48-52.

[36] M. Bauer, R. K. Harris, R. C. Rao, D. C. Apperley, C. A. Rodger, NMR study of desmotropy in Irbesartan, a tetrazole-containing pharmaceutical compound, Journal of the Chemical Society, Perkin Transactions 2, (1998) 475-482.

[37] B. Efron, Bootstrap Methods: Another Look at the Jackknife, Ann. Statist., 7 (1979) 1-26.

[38] D. Bochicchio, E. Panizon, R. Ferrando, L. Monticelli, G. Rossi, Calculating the free energy of transfer of small solutes into a model lipid membrane: Comparison between metadynamics and umbrella sampling, J. Chem. Phys, 143 (2015) 144108.

[39] C. Fotakis, G. Megariotis, D. Christodouleas, E. Kritsi, P. Zoumpoulakis, D. Ntountaniotis, M. Zervou, C. Potamitis, A. Hodzic, G. Pabst, M. Rappolt, G. Mali, J. Baldus, C. Glaubitz, M.G. Papadopoulos, A. Afantitis, G. Melagraki, T. Mavromoustakos, Comparative study of the AT(1) receptor prodrug antagonist candesartan cilexetil with other sartans on the interactions with membrane bilayers, Biochim. Biophys. Acta, 1818 (2012) 3107-3120.

[40] E.F. Pettersen, T.D. Goddard, C.C. Huang, G.S. Couch, D.M. Greenblatt, E.C. Meng, T.E. Ferrin, UCSF Chimera--a visualization system for exploratory research and analysis, J. Comput. Chem., 25 (2004) 1605-1612.

[41] W.X. de Paula, A.M. Denadai, M.M. Santoro, A.N. Braga, R.A. Santos, R.D. Sinisterra, Supramolecular interactions between losartan and hydroxypropyl-beta-CD: ESI mass-spectrometry, NMR techniques, phase solubility, isothermal

titration calorimetry and anti-hypertensive studies, Int. J. Pharm., 404 (2011) 116-123.

[42] S. Lee, S. Kwon, H.J. Shin, E. Cho, K.R. Lee, S. Jung, Electrospray ionization mass spectrometric analysis of noncovalent complexes of hydroxypropyl-β-cyclodextrin and β-cyclodextrin with progesterone, Bull. Korean Chem. Soc., 30 (2009) 1864-1866.

Table legends

Table 1: Thermal parameters for different DPPC samples studied.

Samples	Pretransition state		Transition state	
	ΔH (J/g)	**T_{pre} (ºC)**	**ΔH (J/g)**	**T_m (ºC)**
DPPC	6.3	35	41.8	41.2
DPPC/IRB (80:20)			40.8	39.7
DPPC/HP-β-CD (80:20)	3.9	33	34.0	39.3
DPPC/[IRB–HP-β-CD] complex added (80:20)			38.2	39.3
DPPC/[IRB–HP-β-CD] (80:20)			41.0	39.8

FIGURES LEGENDS

Figure 1: Irbesartan, DPPC and 2-Hydroxypropyl-β-Cyclodextrin (HP-β-CD). The labeled numbers are used for the structure identification in NMR studies.

Figure 2: (left) IRB complex with CD during the preparation is within the lipid bilayers (right) IRB complex with CD is provided outside from the lipid bilayers. These two different preparations potentially can lead to two different ways that IRB interacts with lipid bilayers after its release.

Figure 3: SAXS experiments on (A) pure DPPC bilayers; (B) DPPC/IRB bilayers (80:20); (C) DPPC/HP-β-CD bilayers (80:20); (D) DPPC MLV dispersion with [IRB/HP-β-CD] complex added (80:20); and (E) DPPC/[IRB/HP-β-CD] bilayers (80:20).

Figure 4: D-spacings versus temperature for pure DPPC bilayers (blue circles); DPPC/IRB bilayers (80:20) (black triangles); DPPC/HP-β-CD bilayers (80:20) (red squares); and DPPC MLV dispersion with [IRB/HP-β-CD] added (80:20) (green diamonds). Note, DPPC/[IRB/HP-β-CD] bilayers (80:20) display only uncorrelated (unbound) bilayers.

Figure 5: ^{13}C CP/MAS spectra of the samples used in our studies recorded at 45 ^{o}C and using Bruker 600 MHz spectrometer. Asterisks designate peaks originating from HP-β-CD.

Figure 6: 10 kHz CP (blue) versus red MAS spectrum, at 15 ^{o}C of the sample DPPC/ HP-β-CD (x=0.20). The MAS spectrum shows additional signals which can be assigned to HP-β-CD.

Figure 7: A) Snapshot of one IRB molecule in the DPPC bilayer. The green contour is employed for a better visualization of the molecule in question. **B)** Density profiles of water, DPPC and IRB molecules (12.2 mol%) along the Z-axis which is perpendicular to the two monolayers of the membrane. **C)** Graphical representation of IRB–HP-β-CD in the DPPC membrane in contact with an extended water phase. The IRB and CD derivative are depicted with blue and black colour, respectively. **D)** Density profiles of water, DPPC, IRB and IRB–HP-β-CD along the Z-axis during the last 0.25 μs of an MD simulation.

Figure 8: Representative conformation of IRB in the DPPC bilayer.

Figure 9. Electrospray mass spectrum in negative ion mode of (A) HP-β-CD and (B) IRB–HP-β-CD complex.

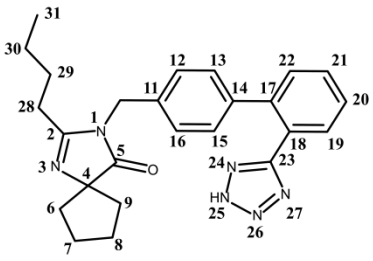

Irbesartan

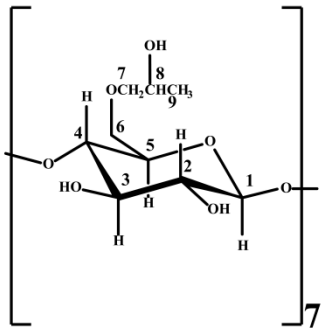

β-D-glycopyranose unit

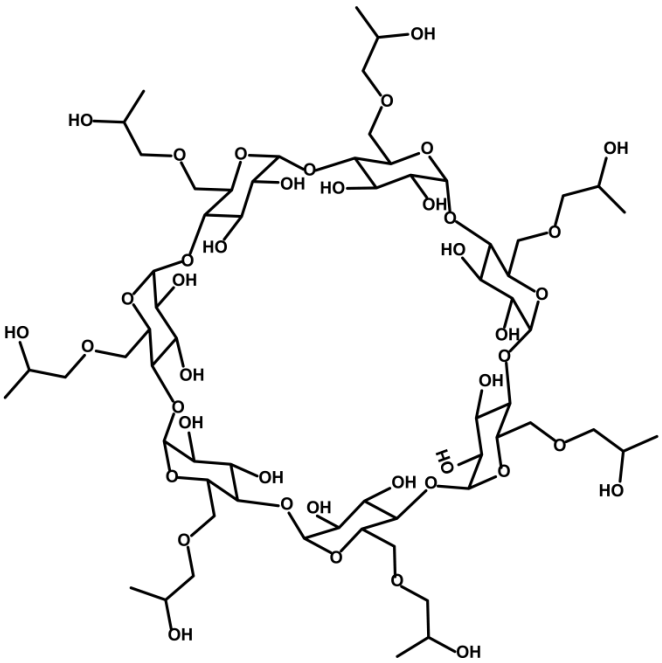

2-hydroxypropyl-β-cyclodextrin

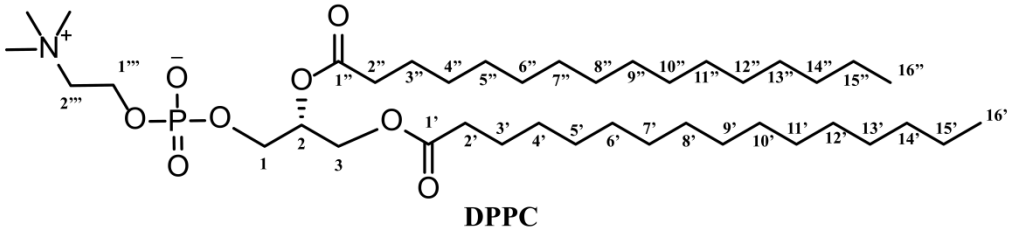

DPPC

Figure 1.

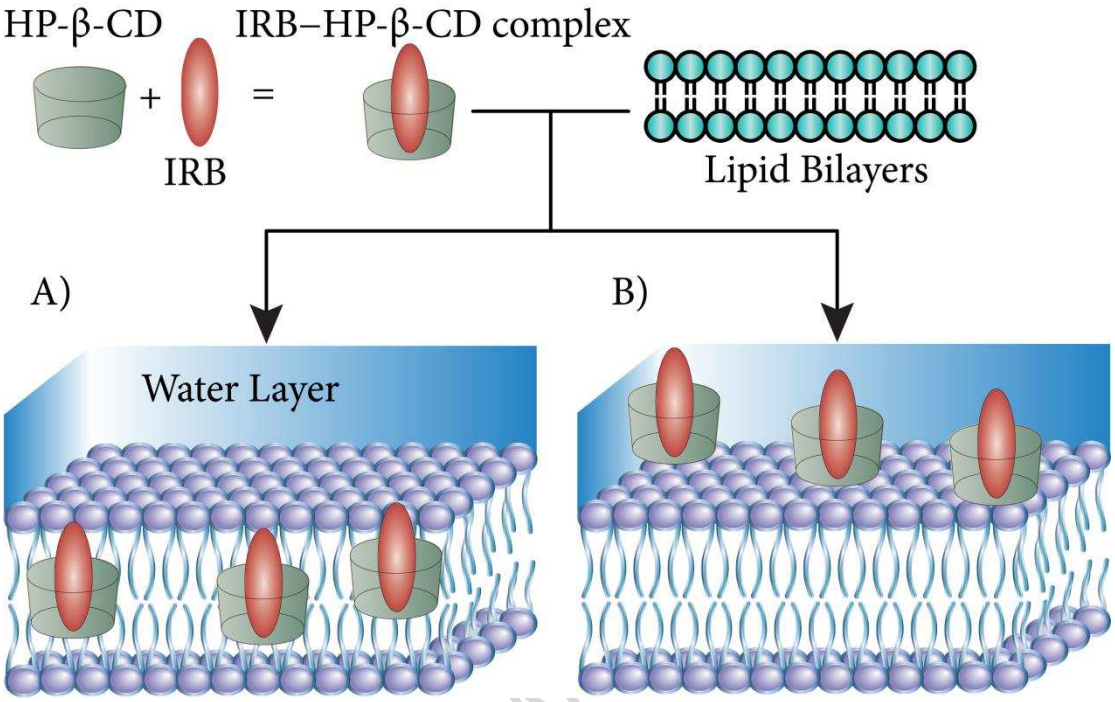

Figure 2

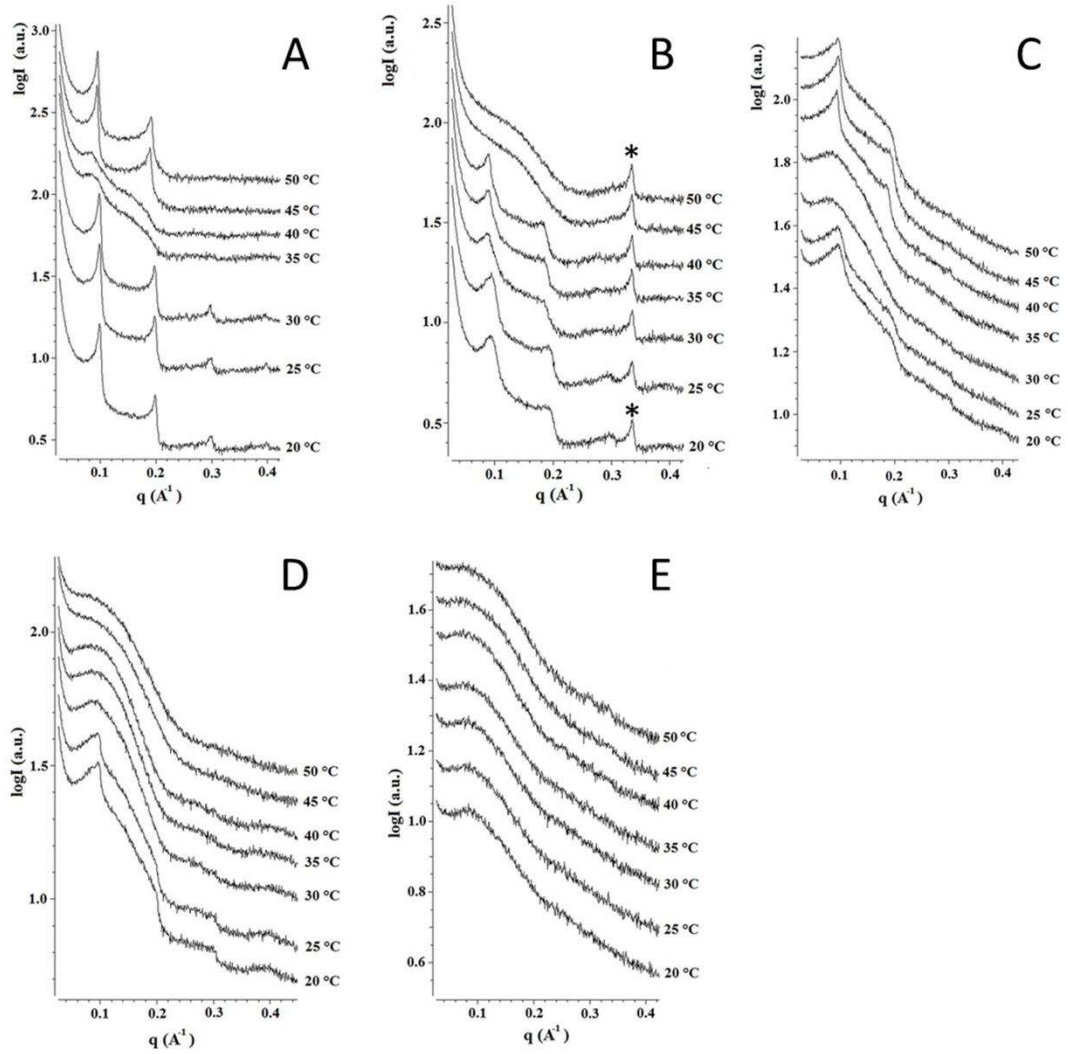

Figure 3.

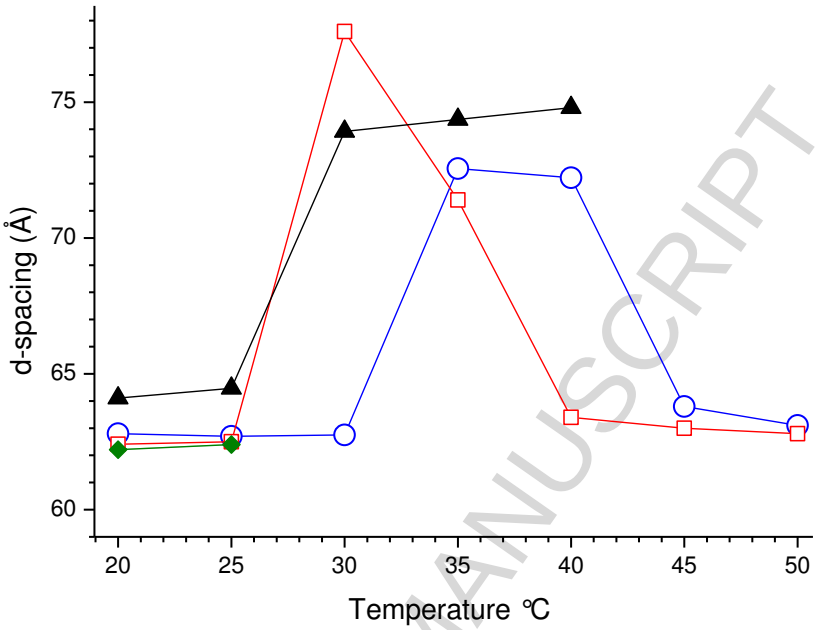

Figure 4.

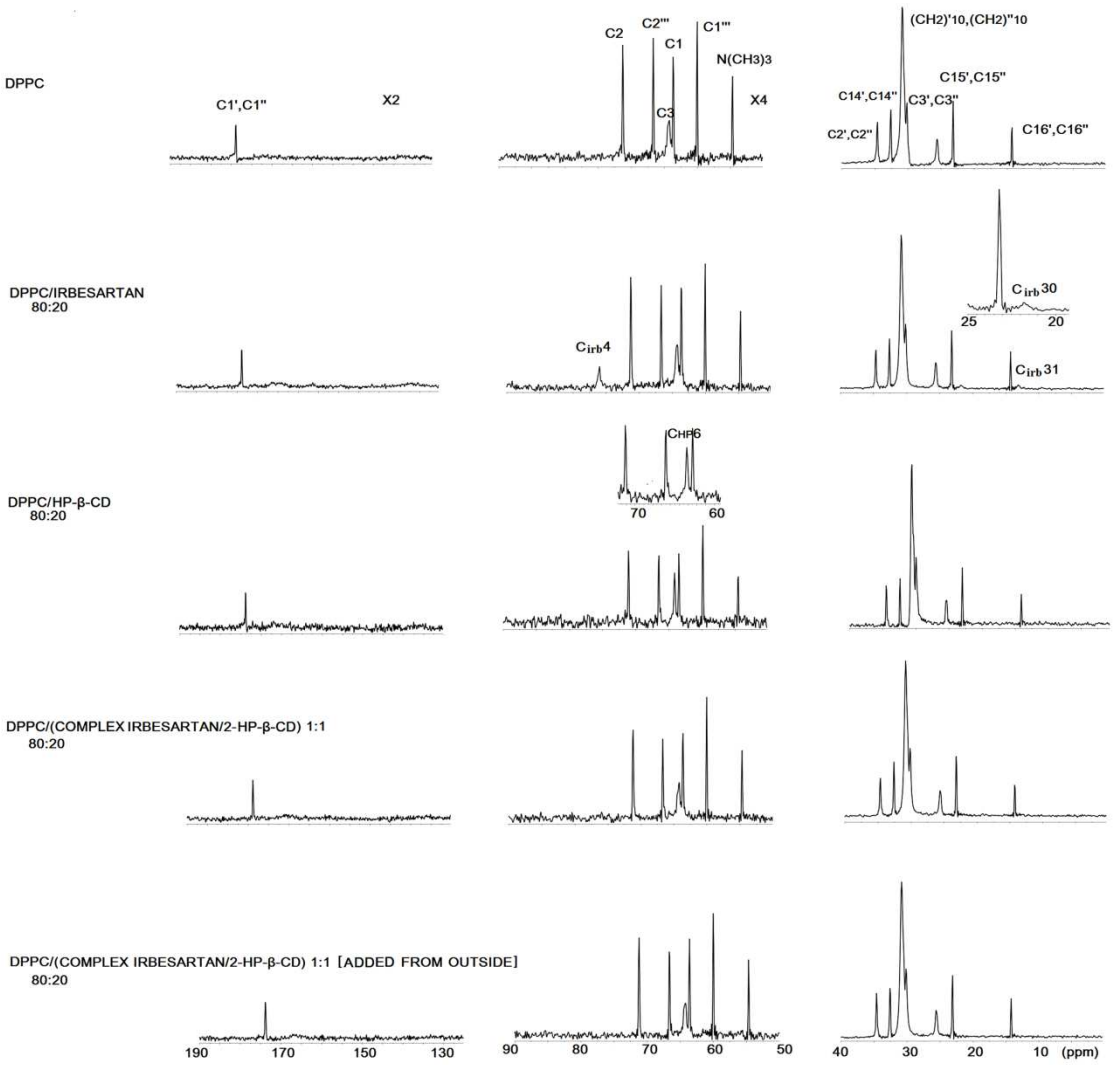

Figure 5.

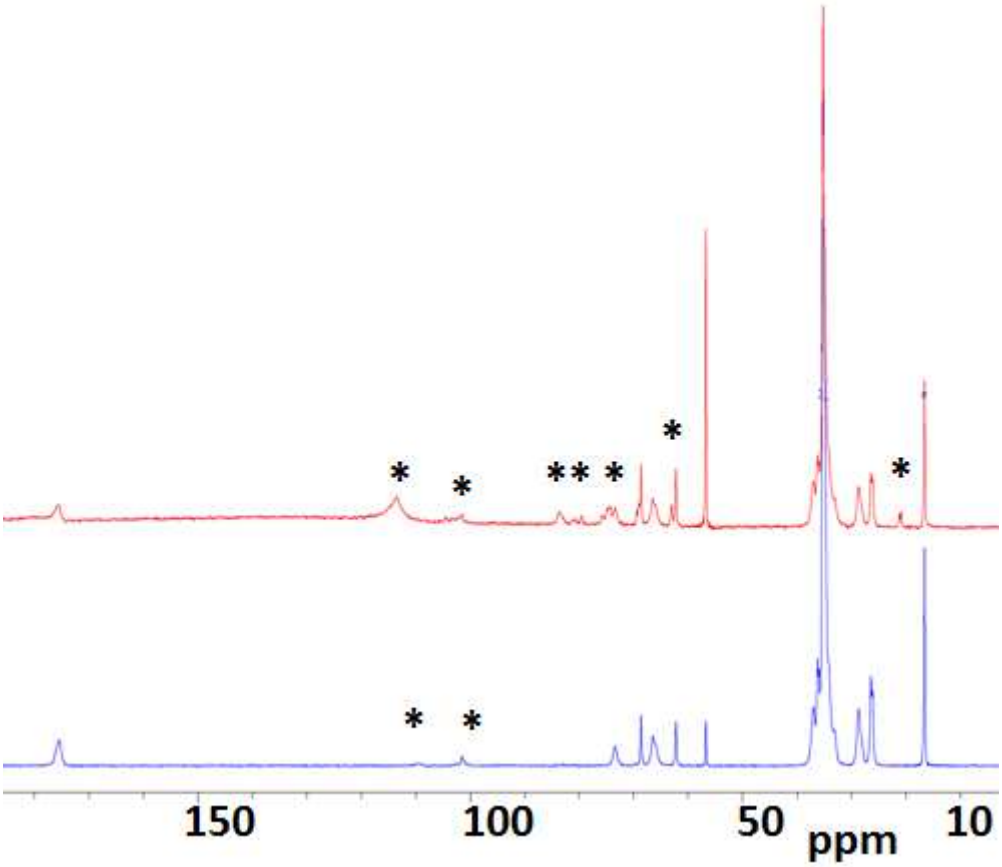

Figure 6.

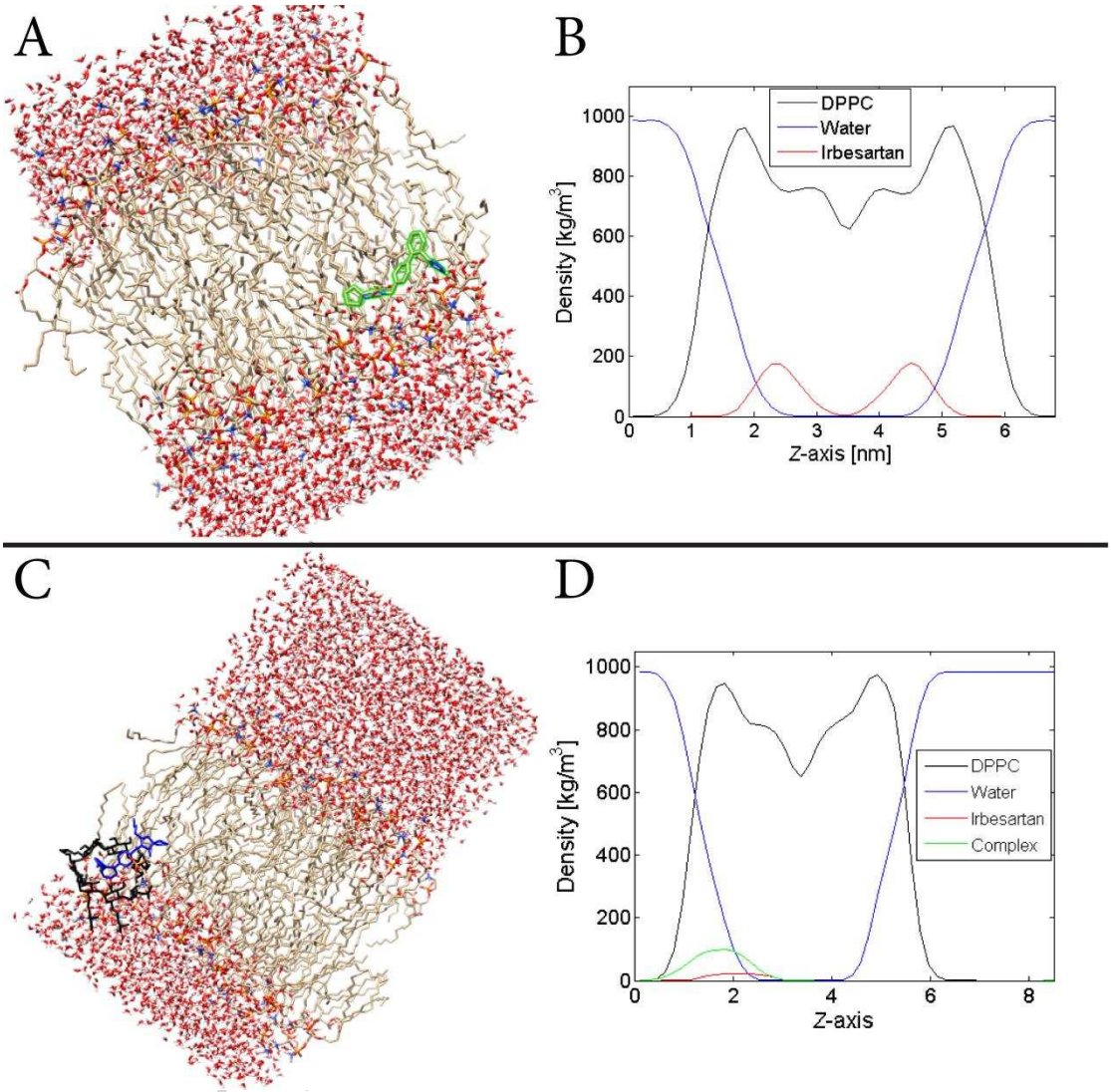

Figure 7

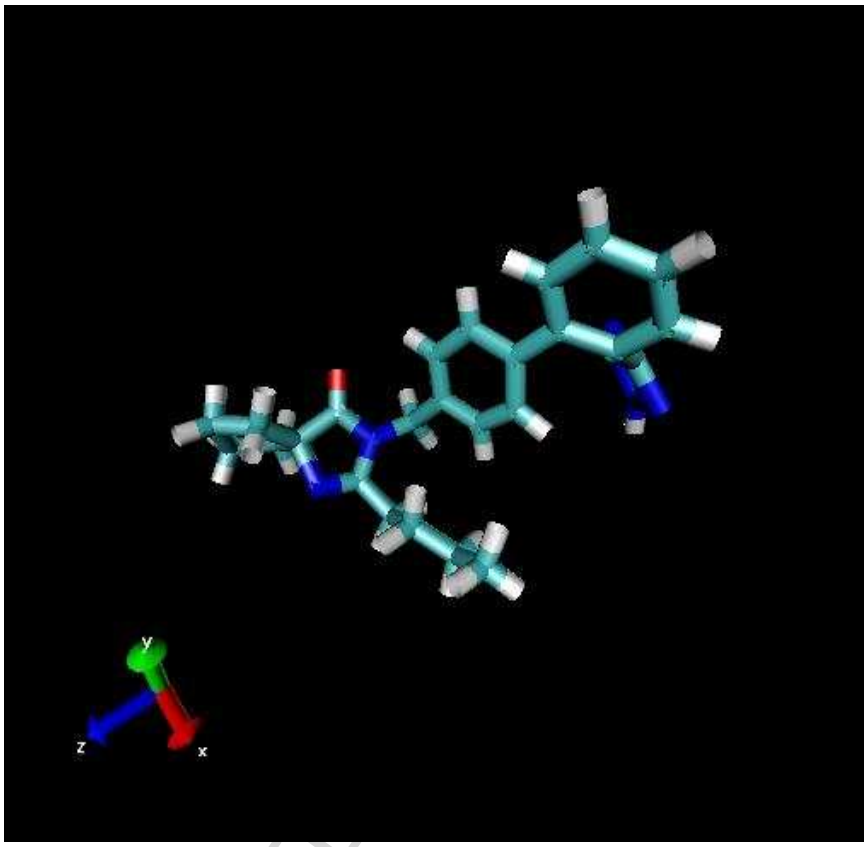

Figure 8.

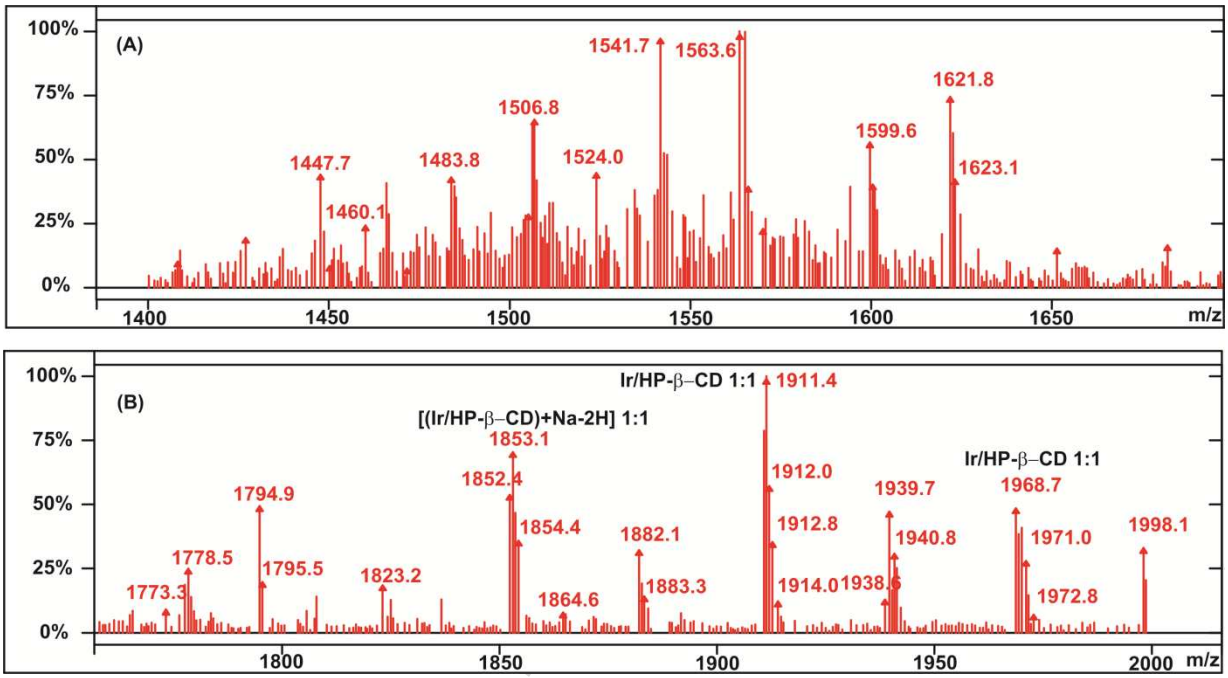

Figure 9.

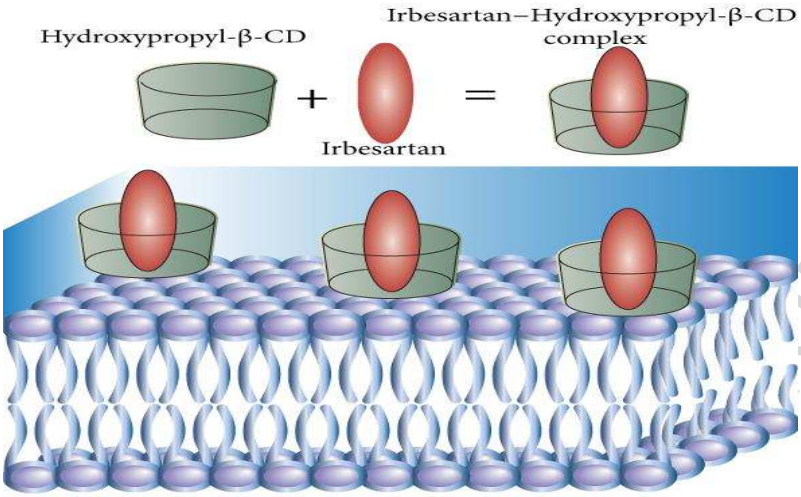

Graphical Abstract

Highlights

- Investigation of a drug-cyclodextrin-lipid bilayer system.
- Irbesartan insertion in DPPC bilayers modifies their thermal profile.
- MD experiments provide information on the localization of irbesartan in DPPC.